

MEASURING AND ENHANCING THE VISUAL CONTENT OF POLARIMETRIC SYNTHETIC APERTURE RADAR DECOMPOSITIONS

Ulilé Indeque *

Laboratório de Computação Científica
e Análise Numérica
Universidade Federal de Alagoas, Brazil

Alejandro C. Frery †

School of Mathematics and Statistics
Victoria University of Wellington, New Zealand

ABSTRACT

Polarimetric Synthetic Aperture Radar images provide important information about the scene under observation. There are several ways in which such information can be extracted, among them the visualization of polarimetric decompositions. A polarimetric decomposition extracts features which, in principle, are related to basic components of the scene. Its visualization depicts such components as variations in hue and intensity, but its interpretation may be hampered by low contrast. Several image enhancement techniques may be applied to improve such a representation, but they may hamper the information contents. We propose an approach for such enhancement based on the visual content that does not alter the interpretability of color images based on polarimetric decompositions and, at the same time, enhances the user's ability to extract visual information. The technique also provides a quantitative measure of such visual content.

Index Terms— Image enhancement; Information content; Polarimetric decompositions; SAR Polarimetry; Stochastic distances.

1. INTRODUCTION

Polarimetric Synthetic Aperture Radar (PolSAR) images have a prominent role in remote sensing (Cloude, 2010; Lee and Pottier, 2009). Such images are formed by the return from the scene in several combinations of transmitting and receiving polarization of the electromagnetic waves.

The observation in each pixel of a fully polarimetric image is a 2×2 complex-valued matrix:

$$\mathbf{S}' = \begin{pmatrix} S_{\text{HH}} & S_{\text{HV}} \\ S_{\text{VH}} & S_{\text{VV}} \end{pmatrix}, \quad (1)$$

in which S_{ij} is a complex value, and i and j are any of the two possible orientations: H (horizontal) or V (vertical). Under the reciprocity principle, $S_{\text{HV}} = S_{\text{VH}}$, so the information

in the scattering matrix (1) can be encoded in the scattering vector

$$\mathbf{S} = \begin{pmatrix} S_{\text{HH}} \\ S_{\text{HV}} \\ S_{\text{VV}} \end{pmatrix} \quad (2)$$

without loss of information.

More often than not, users employ multilooked images, in which L ideally independent observations are averaged:

$$\mathbf{Z} = \frac{1}{L} \sum_{\ell=1}^L \mathbf{S}(\ell) \mathbf{S}^\dagger(\ell), \quad (3)$$

where “ \dagger ” denotes the transpose of the complex conjugate. With this, the multilook observation in each pixel has the form

$$\mathbf{Z} = \begin{pmatrix} I_{\text{HH}} & \text{Cov}(S_{\text{HH}}, S_{\text{HV}}) & \text{Cov}(S_{\text{HH}}, S_{\text{VV}}) \\ \text{Cov}^*(S_{\text{HH}}, S_{\text{HV}}) & I_{\text{HV}} & \text{Cov}(S_{\text{HV}}, S_{\text{VV}}) \\ \text{Cov}^*(S_{\text{HH}}, S_{\text{VV}}) & \text{Cov}^*(S_{\text{HV}}, S_{\text{VV}}) & I_{\text{VV}} \end{pmatrix}, \quad (4)$$

in which “ $*$ ” denotes the complex conjugate, the diagonal elements are intensities, and the off-diagonal entries are the complex covariances between channels. Except from a scale, (4) is known as the coherence matrix. There are other forms of storing the polarimetric return, among them the Pauli and the Kennaugh decompositions. These representations are related, and it is relatively simple to transform one into another.

It is not possible to visualize directly observations of the form (4), as they belong to $\mathbb{R}_+^3 \times \mathbb{C}^3$, i.e., they are nine-dimensional objects. Such observations encode valuable information from the target, and it is desirable to extract and visualize it. Such extraction can be accomplished using Decomposition Theorems.

PolSAR decomposition consists in retrieving the components which gave rise to each observation. The purpose of such operation is to identify the average scattering mechanism within each pixel.

Chen et al. (2014) discuss the general additive decomposition framework

$$\mathbf{Z} = \sum_i^N \pi_i \mathbf{Z}^{(i)}, \quad (5)$$

*Email: ui@laccan.ufal.br

†Email: alejandro.frery@vuw.ac.nz

in which $Z^{(i)}$ is a prototypical scattering, π_i the relative amount with which it contributes to the observation Z , and N is the number of components in the resolution cell. Alternatively, Ratha et al. (2020) discuss a multiplicative rather than additive approach to this problem.

There are several well-known prototypical scatterers, whose form depends on the target. Among them, we mention the volume, double bounce, odd bounce, and helix. Their coefficients in an observation depends both on the target and on the sensing system conditions.

We are interested in decomposition theorems that naturally lead to visualization, i.e., that produce three components that can be mapped onto the red, green, and blue channels. Examples of such decompositions are Barnes-Holmes, Pauli, Krogager, and Hyunen.

The dynamic range of the components values is typically very large, and the user has to choose how to map them into, usually, the $[0, 255]$ interval in order to produce a pseudocolor image. Typical mappings are the linear, the trimmed linear, and the equalization. The linear mapping usually produces almost black images, while the trimmed linear requires stipulating a lower and upper bound. Equalization has the advantage of producing values in $[0, 1]$ which can be easily converted to $[0, 255]$, but it may lead to color which are not related to the original ones.

A very popular visual enhancement technique is the spectral decorrelation. It consists in computing the principal components of the original values (the decorrelation step), enhancing, and applying the inverse rotation. This operation tends to produce crisp images with exaggerated contrast.

Tsagaris and Anastassopoulos (2005) proposed a technique for measuring the information content of color images with the Kullback-Leibler divergence between the observed and ideal histograms of the pixel values in the CIELAB color space. This approach also allows improving an image's contrast by maximizing its realizable color information while retaining the chroma and hue.

In this paper, we propose a modified approach to measuring the visual information content in pseudocolor compositions obtained from decomposition theorems. We also use our approach to enhance them without altering the information they encode.

2. METHODOLOGY

The ideal image's values occupy regularly the CIELab color space. Each pixel in an image in CIELab representation is of the form $I = (L, a, b)$, where $L \in [0, 100]$ is the lightness (darkest to brightest), $a \in [-200, 200]$ measures the color component from green to red, and $b \in [-200, 200]$ describes the color component from blue to yellow. This color representation, differently from the RGB and CMYK color spaces, approximates the human vision system. Tsagaris and Anastassopoulos (2005) present and discuss the one-to-one con-

versions between color spaces.

2.1. Proposed approach

The matching histogram technique consists in adjust the histogram of an image to be similar to another referenced image.

Consider two objects I and O , respectively the ideal and original image. The matching histogram function receives two object: the H_{L_I} component as reference and the H_{L_O} interest's object.

The first step is equalization of H_{L_O} . This is done by applying the Empirical Cumulative Distribution Function - ECDF to the data. This function is defined by

$$F(t) = \frac{1}{N} \sum_{j=1}^N I(t_j \leq t), \quad (6)$$

the indicator I is defined as

$$I(t_j \leq t) = \begin{cases} 1, & t_j \leq t \\ 0, & t_j > t. \end{cases} \quad (7)$$

Applying (6) to H_{L_O} , we obtain the equalized image, denoted as eH_{L_O} .

The matching histogram can be obtained using the inverse empirical cumulative distribution function of H_I , applied to eH_{L_O}

$$F_{L_I}^{-1}(eH_{L_O}). \quad (8)$$

From (8), we have as result the histogram of L_O component approximately equal to H_{L_I} . Using this component, we can reconstruct the original image O , replacing H_{L_O} to aH_{L_O} . Finally, we have the enhanced original image formed by $O = (aH_{L_O}, a_I, b_I)$ and converted back to RGB space color $O = (r_O, a_O, b_O)$.

The methodology is outlined in Fig. 1.

2.2. Evaluation Metrics

An important point is to know how efficient the proposed technique is, i.e., a quantitative measure of the closeness of the results to the ideal image.

This can be done by comparing the images histograms. There are several metrics that quantify the similarity between two probability distributions, among them the Kullback-Leibler divergence (Tsagaris and Anastassopoulos, 2005), and the Hellinger, Euclidean, and Canberra distances (Rubel et al., 2021). Tsagaris and Anastassopoulos (2005) used the Kullback-Leibler divergence in their proposal.

Consider the images $p(L, a, b)$ and $q(L, a, b)$. The Kullback-Leibler divergences between the proportions p and

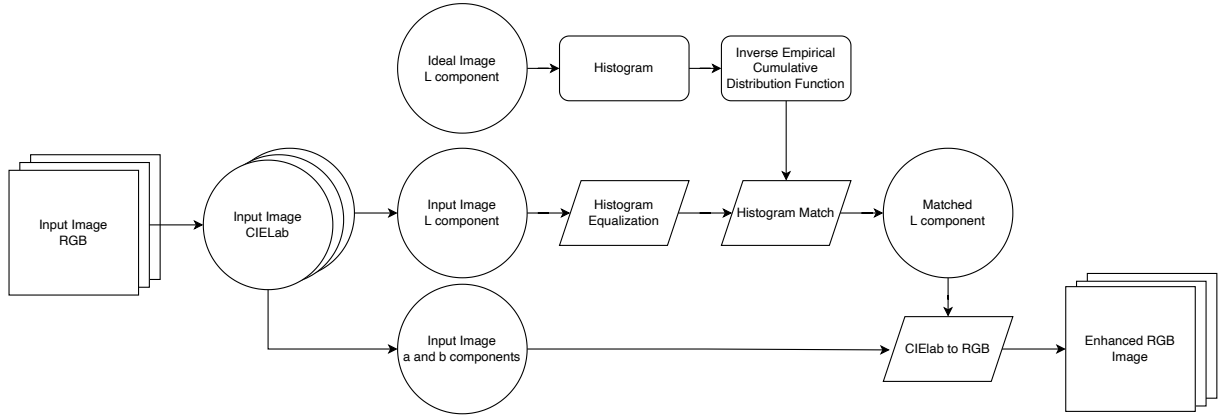


Fig. 1: Outline of the enhancement procedure

q of observations channels in the channels:

$$D_L(p, q) = \sum_L p(L) \log \frac{p(L)}{q(L)}, \quad (9)$$

$$D_a(p, q) = \sum_a p(a) \log \frac{p(a)}{q(a)}, \quad (10)$$

$$D_b(p, q) = \sum_b p(b) \log \frac{p(b)}{q(b)}. \quad (11)$$

The authors then propose adding these components divergences to obtain a measure of the difference between the images. The Kullback-Leibler divergence is not necessary symmetric, and requires computing a ratio in which the denominator may be zero, and the logarithm of a quantity that may be zero.

The Hellinger distance is a widely used measure which does not have the problems mentioned above. It is defined as

$$H(p, q) = \frac{1}{2} \sqrt{\sum_{j=1}^k (\sqrt{p_j} - \sqrt{q_j})^2} \quad (12)$$

for each component as in Eqs. (9)–(11). Rubel et al. (2021) computed the Hellinger distance along with other seven metrics, considering some factors such as complexity and the relationship with the amount of noise, and the Hellinger distance presented consistent and acceptable results. We used the Hellinger distance to compute the dissimilarity between the images and the ideal signal.

3. RESULTS

Fig. 2 shows an original Pauli decomposition and a zoom (Figs. 2a and 2e), the result of applying contrast enhancement by spectral decorrelation (Figs. 2b and 2f), the version with equalized bands (Fig. 2c and 2g), and the result of applying contrast improvement in the CIELab space (Figs. 2d

and 2h). The differences are noticeable. While the three first have crisp and highly saturated colors, the last one is more realistic while preserving the hue. In particular, the image enhanced by decorrelation (Figs. 2b and 2f) produces colors which are not interpretable in terms of a Pauli decomposition.

We computed the distances of these images to the ideal one using (12). The results are: $H(\text{Ideal}, \text{Improved}) = 0.330$, $H(\text{Ideal}, \text{Equalized}) = 0.186$, $H(\text{Ideal}, \text{Decorrelated}) = 0.299$.

4. DISCUSSION

We have presented an image enhancement technique which preserves the chroma and hue. The transformation is based on pixel-wise operations, and requires a reference image that is fixed for every application and input image size. The results suggest that preserving the chroma and hue is a relevant feature, in particular for the visual interpretation of polarimetric decompositions.

We suggest adding this transformation, and its associated measure of performance, to visualization pipelines.

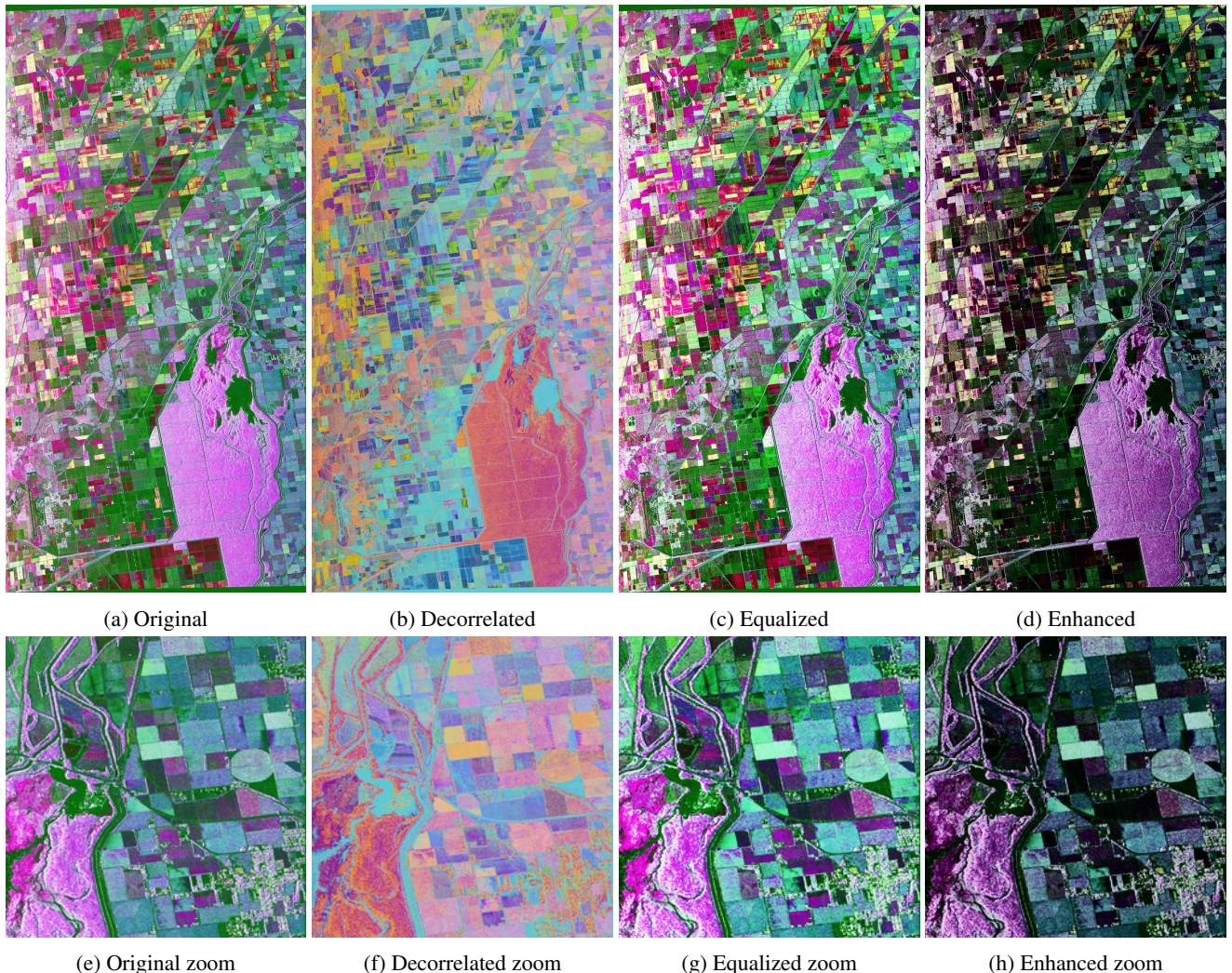


Fig. 2: Original Pauli, enhanced by decorrelation, equalized, and enhanced images, along with their zooms

References

- S. W. Chen, Y. Z. Li, X. S. Wang, S. P. Xiao, and M. Sato, “Modeling and interpretation of scattering mechanisms in polarimetric synthetic aperture radar: Advances and perspectives,” *IEEE Signal Processing Magazine*, vol. 31, no. 4, pp. 79–89, July 2014.

S. R. Cloude, *Polarisation: Applications in Remote Sensing*. Oxford University Press, 2010.

J.-S. Lee and E. Pottier, *Polarimetric Radar Imaging: From Basics to Applications*. Boca Raton: CRC, 2009.

D. Ratha, E. Pottier, A. Bhattacharya, and A. C. Frery, “A Pol-SAR scattering power factorization framework and novel roll-invariant parameters based unsupervised classification scheme using a geodesic distance,” *IEEE Transactions on Geoscience and Remote Sensing*, vol. 51, no. 1, pp. 1–12, Jan. 2013.

Geoscience and Remote Sensing, vol. 58, no. 5, pp. 3509–3525, May 2020.

O. Rubel, R. Tsekhnystro, V. Lukin, and K. Egiazarian,
 “Benchmark of similar blocks search under noisy conditions,” vol. 2021, 04 2021.

V. Tsagaris and V. Anastassopoulos, "Assessing information content in color images," *Journal of Electronic Imaging*, vol. 14, no. 4, p. 043007, Oct. 2005.